PII S0016-7037(02)01085-2

History and origin of aubrites

S. Lorenzetti,[1,*] O. Eugster,[1] H. Busemann,[1] K. Marti,[2] T. H. Burbine,[3] and T. McCoy[3]

[1]Physikalisches Institut, University of Bern, Sidlerstrasse 5, 3012 Bern, Switzerland
[2]University of California, San Diego, Chemistry, 9500 Gilman Drive, La Jolla, CA 92093-0317, USA
[3]Smithsonian Institution, Dept. of Mineral Sciences MRC NHB-119, Washington DC 20560, USA

Abstract—The cosmic ray exposure (CRE) ages of aubrites are among the longest of stone meteorites. New aubrites have been recovered in Antarctica, and these meteorites permit a substantial extension of the database on CRE ages, compositional characteristics, and regolith histories. We report He, Ne, and Ar isotopic abundances of nine aubrites and discuss the compositional data, the CRE ages, and regolith histories of this class of achondrites. A Ne three-isotope correlation reveals a solar-type ratio of $^{20}Ne/^{22}Ne = 12.1$, which is distinct from the present solar wind composition and lower than most ratios observed on the lunar surface. For some aubrites, the cosmic ray-produced noble gas abundances include components produced on the surface of the parent object. The Kr isotopic systematics reveal significant neutron-capture-produced excesses in four aubrites, which is consistent with Sm and Gd isotopic anomalies previously documented in some aubrites. The nominal CRE ages confirm a non-uniform distribution of exposure times, but the evidence for a CRE age cluster appears doubtful. Six meteorites are regolith breccias with solar-type noble gases, and the observed neutron effects indicate a regolith history. ALH aubrites, which were recovered from the same location and are considered to represent a multiple fall, yield differing nominal CRE ages and, if paired, document distinct precompaction histories. *Copyright © 2003 Elsevier Science Ltd*

1. INTRODUCTION

The enstatite meteorites have long been of interest because of their reduced mineral composition and variable metal abundances (e.g., Mason, 1962). The composition of metal, schreibersite, and perryite was studied by Wasson and Wai (1970) to assess the origins of aubrites (the member name used for enstatite achondrites) and enstatite chondrites. Watters and Prinz (1979) concluded that it is not clear whether aubrites represent nebular condensate or igneous differentiates. They also noted that the enstatite meteorite Happy Canyon (EL6) shows compositional similarities to aubrites, including negative Eu anomalies, which suggest an origin by fractional crystallization. An igneous history of the aubrite parent asteroid was inferred from the study of the Norton County meteorite (Okada et al., 1988), while evidence for an impact origin was found in Shallowater (Keil et al., 1989). The oxygen as well as nitrogen isotopic systematics distinguish them from other meteorites (Clayton et al., 1984; Murty and Marti, 1990). Oxygen isotopic signatures of enstatite meteorites plot close to the terrestrial fractionation line (Clayton et al., 1984; Newton et al., 2000) and document that the source is distinct from chondritic parent asteroids. The O signatures of enstatite meteorites also plot close to terrestrial and lunar pyroxenes (Clayton et al., 1984). Oxygen isotope ratios, recently determined in 14 aubrites by Newton et al. (2000), confirm signatures close to the terrestrial fractionation line (TFL), but at least four aubrites have $\Delta^{17}O$ signatures offset from the TFL, indicating chondritic or other inclusions. The nitrogen isotopic signatures of aubrites, however, are distinct from those in indigenous lunar rocks (Mathew and Marti, 2001). The $^{35}Cl(n,\gamma\beta)$ neutron-capture reactions

may affect the ^{36}Ar spallation components. Accordingly, $^{36}Ar/^{38}Ar$ ratios of ~7 were observed in stepped-heating studies of the enstatite chondrite Abee (Wacker, 1982).

The cosmic ray exposure (CRE) age of Norton County, the first measured stony meteorite (Begemann et al., 1957), yields the longest currently known exposure time of a stone meteorite. Gaffey et al. (1992) suggested a link between aubrites, near-Earth asteroid 3103, and E-type asteroids of the Hungaria family, based on spectral matches and orbital dynamics considerations. Moreover, the orbital elements of Apollo object 3103 (Eger) are consistent with long collisional lifetimes. Crabb and Anders (1981) found that exposure ages of enstatite meteorites show a trend, E4 < E6 < aubrites, while Patzer and Schultz (2001) conclude that there is no systematic trend in E chondrites either for subgroups or for petrologic types.

The first systematics on the exposure ages of aubrites were obtained by Eberhardt et al. (1965a). These workers noted a cluster of exposure ages at ~40 Ma and that some of the aubrites show the presence of solar wind (SW) gases. In fact, the high relative occurrence of SW-containing meteorites among the enstatite achondrites is a major reason for a detailed examination of a regolith exposure history on their parent asteroid (Graf and Marti, 1992). Further, the occurrence of chondritic inclusions in the Cumberland Falls achondrite (Mason, 1962) and the evidence for a planetesimal impact in the Shallowater meteorite also are indicative of regolith processes. Thermal neutron fluxes in Norton County and Shallowater were reported by Bogard et al. (1995). Large isotopic anomalies in Sm and Gd, due to neutron-capture effects, were reported in five aubrites (Hidaka et al., 1999). The inferred neutron fluences compare to those observed in lunar samples and indicate regolith histories. A comprehensive study of CRE histories of aubrites and of the parent body regolith history appears appropriate at this time, since a number of new aubrites have been

recovered in Antarctica (ALH 84024, EET 90033, EET 90757, LEW 87007, QUE 97289, QUE 97348, and Y 793592). A goal of this work is to integrate CRE ages, SW loading, regolith data, and other mineralogic or petrologic observations. Preliminary data on the CRE ages reported in this work have been published in abstracts (Lorenzetti and Eugster, 2000; Lorenzetti et al., 2001).

2. EXPERIMENTAL METHODS

The investigated samples were crushed in a stainless steel mortar to a grain size of $< 750~\mu$m to get an uniform mixture and then split in two parts, one for the chemical analyses, the other one for noble gas measurements.

2.1. Chemistry

We determined the bulk chemical composition of ALH 84018, ALH 84024, EET 90757, EET 90033, and LEW 87007 by melting a ~50-mg aliquot of each. Samples were melted in a Deltech vertical mixing furnace at 1550°C for 5 min in a graphite crucible wedged on the end of a sealed alumina tube. The short run time, graphite crucible, and sealed container prevented volatilization and/or oxidation of the samples. The fused beads were quenched in air, resulting in glassy-to-microcrystalline textures. Compositions were measured by averaging 20 to 40 individual analyses that each used a 40-μm rastered beam on the JEOL JXA-8900R electron microprobe at the Smithsonian Institution. Oxygen was calculated by stoichiometry for all elements except Fe, Ni, Cr, and S.

The paired QUE 97289/97348 meteorites are terrestrially weathered, and we could not use the same technique to derive their bulk composition. X-ray compositional maps for the QUE samples (QUE 97289 and 97348) were collected for 11 elements (Al, Ca, Cr, Fe, K, Mg, Mn, Na, P, S, and Si) using the scanning electron microscope. From these, we computed area percentages for daubréelite, enstatite, feldspar, metallic iron, and weathering products (assumed to be FeOOH), silica, and schreibersite. The percentages were averaged for the two thin sections, and weight percents were calculated using average densities (Keil, 1968). We estimated that 80% of the metallic iron had been converted to terrestrial FeOOH. The bulk compositions were determined by multiplying the weight percents of the various minerals, and the compositions of each mineral phase were measured using the electron microprobe.

2.2. Noble Gas Mass Spectrometry

2.2.1. He, Ne, and Ar

All investigated samples were interior chips without fusion crust. Before the noble gas analyses, the samples were heated at ~100°C for 1 week in the extraction system to remove atmospheric gases. The noble gases were extracted at 1700°C, and for each sample a second extraction at 1740°C was made. The samples were measured according to procedures discussed by Eugster et al. (1993).

2.2.2. Kr

The heavy noble gas Kr has been measured in the aubrites Cumberland Falls, Mayo Belwa, Mount Egerton, Norton County, and Shallowater. These analyses are part of an extended study on the composition of the trapped heavy noble gases in achondrites (Busemann and Eugster, 2002). We report the excesses of ^{80}Kr and ^{82}Kr from neutron-capture in ^{79}Br and ^{81}Br, respectively. The ^{79}Br (n, $\gamma\beta$) ^{80}Kr reactions are predominantly due to epithermal neutrons (Marti et al., 1966).

3. RESULTS

We first provide brief descriptions of the meteorites and then present the noble gas isotopic abundances in the investigated meteorites and adopted chemical compositions, which are required to calculate production rates for cosmogenic noble gases and to derive radiogenic ages. Most of the measured aubrites (ALH 84007, ALH 84008, ALH 84011, ALH 84024, Aubres, Bustee, EET 90033, EET 90757, LEW 87007, Mayo Belwa, Norton County, Peña Blanca Spring, Pesyanoe, and Y 793592) have roughly similar mineralogy (Watters and Prinz, 1979), consisting predominately of enstatite (~80–95 vol.%) with minor feldspar, sulfides, metallic iron, diopside, and forsterite.

3.1. Petrographic and Chemical Data

Although most investigated aubrites are breccias, they differ significantly in the degree of brecciation and shock blackening. Most of them are finely brecciated (e.g., Khor Temiki), with clasts typically a few millimeters in diameter. However, coarse clasts and individual silicate inclusions reaching 45 mm in size (Mason, 1962) are found in some aubrites; in Peña Blanca Spring, such inclusions reach up to 10 cm (Lonsdale, 1947; this work). Aubrites also vary significantly in their degree of shock-blackening. Mayo Belwa, in particular, is extensively shock-blackened, and approximately one-third of the ALH 84 aubrite pairing group are shock-blackened.

The following paragraphs give petrologic descriptions of each of the aubrites studied in this paper. We reference previous studies for each of the meteorites; however, Smithsonian or Johnson Space Center samples and thin sections of each meteorite (excluding the Japanese ones) were examined to confirm the descriptions.

Two aubrites (ALH 78113, Cumberland Falls) are known to contain chondritic clasts (e.g., Neal and Lipschutz, 1981; Kallemeyn and Wasson, 1985; Lipschutz et al., 1988). The matrices of these meteorites are similar to the brecciated aubrites, consisting of igneous clasts dominated by enstatite. The clasts are chondrule-bearing, rich in metal and sulfide, and sample a group of meteorites not otherwise represented in our collections. The chondritic inclusions in ALH 78113 are much smaller and much sparser than those found in Cumberland Falls.

Aubres is a whitish rock and contains 97 vol.% enstatite (Watters and Prinz, 1979), with minor plagioclase, diopside, forsterite, troilite, and metallic iron. The enstatite varies from a fine-grained matrix to grains as large as ~1 cm.

Bishopville is similar to the finely brecciated aubrites in most respects, but is mineralogically unusual in containing a significantly higher abundance of plagioclase (16 vol.%) relative to other known aubrites (Watters and Prinz, 1979).

Mt. Egerton is an unbrecciated meteorite composed of cm-sized enstatite crystals with ~21 wt.% metallic Fe, Ni occurring in the interstices between the large enstatite laths (Casanova et al., 1993). It broke into fragments no larger than 5 cm across on impact with Earth. It is similar in most respects to aubrites and should probably be classified as an aubrite. It is unusual in being unbrecciated and containing a far greater percentage of Fe, Ni metal than other aubrites.

Norton County is the largest recovered aubrite with an estimated mass of 1 ton (Grady, 2000). Norton County is 85 vol.% enstatite and 10% forsterite (Watters and Prinz, 1979), with minor diopside, plagioclase, troilite, and metallic iron. The enstatite varies from a fine-grained matrix to inclusions as large as ~8 cm (Okada et al., 1988).

Pesyanoe is a brecciated aubrite composed almost entirely of

enstatite (90 vol.%) and plagioclase (7%) with accessory diopside (1%) and forsterite (1%).

Recently, an unusual clast was discovered in Pesyanoe (Ivanova et al., 2002). This clast is composed of FeO-rich olivine (Fa14), orthopyroxene (En83Wo3), pigeonite (En78Wo9), and Ti-poor troilite (Keil et al., 1989). It is unclear if this clast is indigenous to the aubrite parent body or has a foreign origin. One of these clasts is composed of FeO-rich olivine (Fa14), orthopyroxene (En84 Wo3), pigeonite (En79 Wo9), and Ti-poor troilite. Another clast is composed of a mixture of plagioclase and silica.

The paired aubrites, QUE 97289 and QUE 97348, exhibit igneous textures and mineralogies consistent with their inclusion in the enstatite meteorite clan, but the material is believed to have formed as impact melts from known enstatite chondrites (McCoy et al., 1995; Burbine et al., 2000). The QUE 97289/97348 meteorites consist predominately of ~1 mm-sized, rounded enstatite grains with abundant feldspar, metal, and sulfides, and their bulk compositions are similar to enstatite chondrites (Table A1).

Shallowater is an unbrecciated aubrite consisting of 80 vol.% orthoenstatite crystals with monomineralic or polymineralic inclusions of twinned low-Ca clinoenstatite, forsterite, plagioclase, metallic Fe, Ni and troilite (Keil et al., 1989). Keil et al. (1989) argued that both the history and parent body of Shallowater are unique, having formed when a solid enstatite chondrite-like planetesimal (the xenolithic inclusions) impacted a completely molten, enstatite-rich parent body (the enstatite-rich host).

Y 793592 is a typical aubrite that is predominately enstatite with minor plagioclase, forsterite, metallic iron, and sulfides (troilite and daubreelite) (Yanai, 1992). The enstatite varies from a fine-grained matrix to grains as large as ~0.6 cm.

Results on the chemical composition of all aubrites are given in Tables A1 and A2 and agree well with the range of bulk aubrite compositions given by Watters and Prinz (1979).

3.2. Noble Gas Data

The results of He, Ne, and Ar analyses are given in Table A3. The literature data given in Table A4 were taken from the compilation of Schultz and Franke (2000). To obtain average values from the various He, Ne, and Ar analyses for the same meteorite, we proceeded in the following way: (1) In general, data published before 1965 were not considered because of uncertainties in the correction for isotopic fractionation effects of Ne (Eberhardt et al., 1966). (2) Aubrite samples with large SW components were not considered, except for Pesyanoe dark. (3) Samples that plot clearly below the $^3He/^{21}Ne$ vs. $^{22}Ne/^{21}Ne$ correlation line (see below) indicate gas loss and were not included in the average value. (4) Samples with ratios $^{22}Ne/^{21}Ne < 1.05$ have uncertainties in the production rates and were not considered. The results of the Kr analysis are given in Table A5 and the excesses due to neutron-capture in Br on isotopes $^{80}Kr_n$ and $^{82}Kr_n$ in four aubrites (Cumberland Falls, Mayo Belwa, Shallowater, and Khor Temiki) in Table 1.

3.3. Solar Ne

Six aubrites (Bustee, EET 90033, Khor Temiki, LEW 87007, Pesyanoe, and Y 793592) contain solar-type light noble gases

Table 1. Cosmogenic and neutron produced Kr in Aubrites.

	$^{83}Kr_c$	$^{80}Kr_n$	
	$10^{-12}cm^3STP/g$		$(^{80}Kr/^{82}Kr)_n$
Cumberland Falls	1.95	15.3	2.8 ± 0.7
Khor Temiki[1]	2.51	0.52	2.4 ± 0.3
Mayo Belwa	3.75	1.5	na
Mt. Egerton	bd	< 0.4	na
Norton County	3.90	< 0.4	na
Shallowater	bd	10.5	1.9 ± 1.5

na - not analyzed; bd - below detection limit. Experimental errors: noble gases ± 15% (1σ); 1) Calculated from data of Eugster et al. (1969).

(Fig. 1) with relative abundances similar to those inferred for the Sun (Anders and Grevesse, 1989). To derive the isotopic signature of solar-type Ne in aubrites, we use the standard three-isotope correlation plot (Fig. 2) with endmembers of trapped and cosmogenic composition. Selected data include only bulk samples and enstatite-rich separates. The observed correlation yields $^{20}Ne/^{22}Ne = 12.1 ± 0.2$ for the trapped component, which is considerably lower than SW-Ne and is closer to solar energetic particle-Ne (SEP-Ne) data (Benkert et al., 1993). This $^{20}Ne/^{22}Ne$ ratio is not only distinct from the modern SW-Ne datum ($^{20}Ne/^{22}Ne = 13.8 ± 0.1$; Benkert et al., 1993), but also differs from long-term average ratios observed
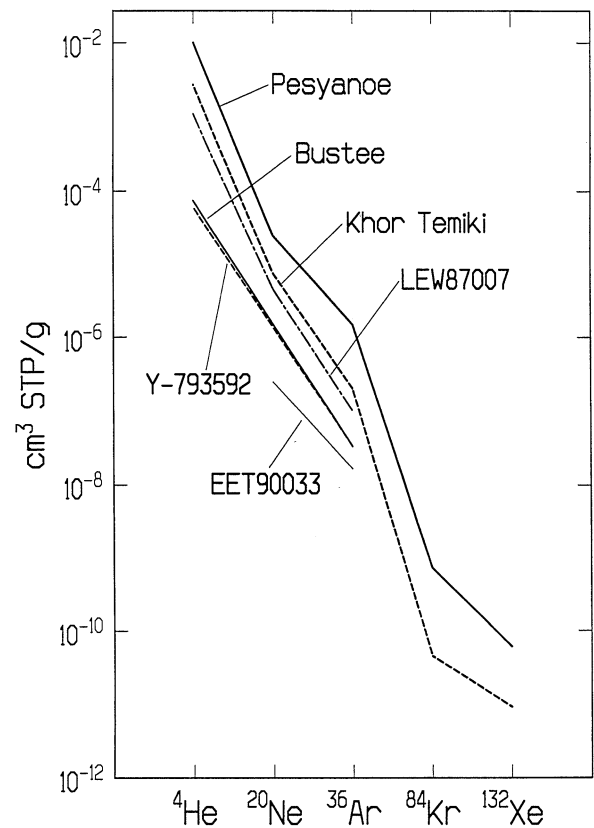

Fig. 1. Trapped noble gas concentrations in the six solar gas-containing aubrites.
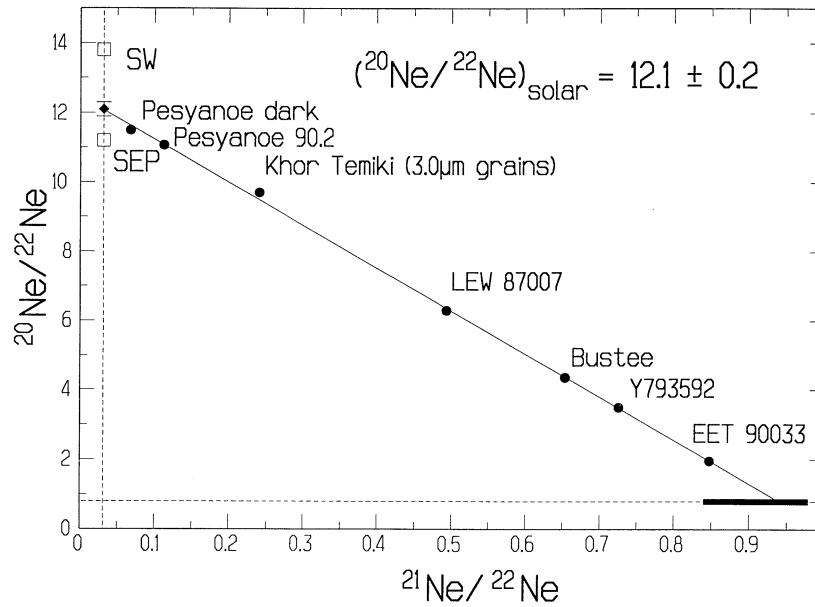
Fig. 2. Neon three-isotope plot for all aubrites with solar gases. Data from this work, except for Khor Temiki (Eberhardt et al., 1966) and Pesyanoe dark (Müller and Zähringer, 1966).

on the lunar surface ($^{20}Ne/^{22}Ne$ = 12.8 ± 0.2) and either documents a distinct mix of SEP and SW Ne components during the irradiation on the aubrite parent body or a different power law spectrum of the superthermal tail of the solar wind, if SEP-Ne ratios represent variable range-energy effects (Mewald et al., 2001). Trapped $^4He/^3He$ ratios obtained for Pesyanoe, Khor Temiki (3-μm sample), and LEW 87007 are higher (~3500) than those observed in the recent solar wind (2350) or on the lunar surface (< 3200) (cf. Eugster et al., 2001).

3.4. Cosmogenic Noble Gases

In the data for Bustee, Khor Temiki (3-μm separate), LEW 87007, Pesyanoe dark, and Y 793592 trapped (tr), ^3He was subtracted from measured ^3He, adopting ^4He_r = 2000 × $10^{-8}cm^3STP/g$, $(^4He/^3He)_{tr}$ = 3500, and $(^4He/^3He)_c$ = 5.2, where (r) is the radiogenic component and (c) the cosmogenic. For all other samples, we adopt ^3He_c = total ^3He. Most aubrites contain some trapped Ne; although the ratio $(^{20}Ne/^{36}Ar)_{tr}$ is generally < 1, we assume Ne_{tr} to be of solar origin and adopt $(^{20}Ne/^{22}Ne)_{tr}$ = 12.1 (Fig. 2) and $(^{20}Ne/^{21}Ne)_{tr}$ = 400. We use a spallation ratio $(^{20}Ne/^{21}Ne)_c$ = 0.9 to calculate $^{21}Ne_c$ abundances. The resulting concentrations are insensitive to these assumptions, since the correction of $^{21}Ne_{tr}$ is always < 3%. Trapped Kr relative isotopic abundances are adopted from Busemann et al. (2000). Table 2 reports the cosmogenic noble gas components in all studied aubrites.

4. DISCUSSION

4.1. The ^{21}Ne Production Rate

Reliable CRE ages for aubrites can be obtained either by the ^{81}Kr-Kr method or from $^{21}Ne_c$ concentrations and in many cases from ^3He_c. Because of low concentrations and inhomogeneous distribution of the elements Ca and Fe, larger uncer-

tainties are encountered with the $^{38}Ar_c$ production rate P_{38}, and CRE ages based on ^{38}Ar are not reported here. The production rates P_3 and P_{21} depend not only on the chemical composition, but also on the shielding properties. Since the chemical composition of aubrites differs from the meteorites for which shielding-dependent production rates are available (for chondrites, see Eugster, 1988; for HED-meteorites, see Eugster and Michel, 1995), production rates need to be evaluated here. The ^{21}Ne production rate (P_{21}) is assumed to have the general form:

$$P_{21} = F\,P'_{21}\,[a(^{22}Ne/^{21}Ne)_c - b]^{-1} \qquad (1)$$

where F is the "composition parameter" for average aubritic chemistry and average shielding conditions, and P'_{21} the production rate for a reference composition (Eugster and Michel, 1995). The "shielding factor" $[a(^{22}Ne/^{21}Ne)_c-b]$ is obtained from the correlation of $^3He/^{21}Ne$ vs. $^{22}Ne/^{21}Ne$ (Fig. 3).

Table A1 lists the chemical compositions of aubrites. Most aubrites are Fe-poor and have quite uniform chemical composition, with average target element abundances given in Table A1 that yield P'_{21} = 0.462 × $10^{-8}cm^3STP/g$, Ma and F = 3.78 ± 0.60. The $^3He/^{21}Ne$ vs. $^{22}Ne/^{21}Ne$ correlation for Fe-poor aubrites in Figure 3 (data in Table 2) fits Eqn. 2:

$$^3He/^{21}Ne = 17.6\,(^{22}Ne/^{21}Ne)_c - 15.9 \qquad (2)$$

Alternatively, the composition parameter F in Eqn. 1 can be calculated from available ^{81}Kr-Kr ages, T_{81}, (Eugster et al., 1969; Miura et al., 1999) from Eqn. 3

$$P_{21} = {}^{21}Ne/T_{81} = F\,P'_{21}[17.6(^{21}Ne/^{21}Ne)_c - 15.9]^{-1} \qquad (3)$$

and we obtain F = 3.52 ± 0.30 (uncertainties in T_{81} included). Although the agreement between the two F values is good, we adopt the F value calibrated with the ^{81}Kr-Kr method, which is composition- and shielding-independent, and obtain the following ^{21}Ne production rate for Fe-poor aubrites:

Table 2. Cosmogenic He, Ne, and Ar in aubrites. Concentrations in $10^{-8}cm^3STP/g$.

	^{3}He	^{21}Ne	^{38}Ar	^{22}Ne/^{21}Ne	References
ALH 78113	35.6	11.5	0.44	1.086	3)
ALH 84007	45.2	14.3	0.19	1.080	4)
ALH 84008	25.9	8.61	0.18	1.095	3)
ALH 84011	36.1	12.2	0.13	1.086	3)
ALH 84024	24.0	8.78	0.12	1.071	5)
Aubres	13.8	5.9	0.12	1.115	3)
Bishopville	91.8	22.4	0.27	1.107	3)
Bustee	88.7	25.8	1.21	1.100	3)
Cumberland Falls Fe-poor	1)	29.0	0.65	1.086	3)
Cumberland Falls Fe-rich	1)	24.5	1.00	1.083	3)
EET 90033	45.0	18.3	0.66	1.064	5)
EET 90757	1)	16.6	0.46	1.105	5)
Khor Temiki enstatite	94.0	24.5	0.19	1.115	3)
LEW 87007	104.5	31.3	1.45	1.073	5)
Mayo Belwa	178	51.8	1.86	1.129	3)
Mt. Egerton	16.3	10.4	0.158	na	6)
Norton County	205	54.4	2.16	1.093	3)
Peña Blanca Springs	119	24.9	0.70	1.181	3)
Pesyanoe light	87.9	19.7	0.46	1.092	3)
Pesyanoe dark	8)	12.2	2)	1.38 ± 0.40	3)
Pesyanoe-92 enstatite crystal 1	78.4	21.7	0.26	1.091	5)
Pesyanoe-92 enstatite crystal 2	77.5	20.7	0.37	1.110	5)
Pesyanoe-90,2	84.4	32.9	2.5	1.081	5)
QUE 97289	71.6	19.6	0.97	1.030	5)
QUE 97348	1)	16.6	1.06	1.023	5)
Shallowater	44.0	7.60	2)	1.190	3)
Y 793592	85.3	34.0	1.03	1.064	5)

Typical experimental errors (2σ mean) are 4% for ^{3}He and ^{21}Ne, 10% for ^{38}Ar, and 1–2% for ^{22}Ne/^{21}Ne, except where indicated; 1) diffusion loss; 2) trapped Ar contribution too high; 3) calculated from data given in Table A4; 4) average calculated for data given in Tables A3 and A4; 5) calculated from data given in Table A3; 6) Miura et al. (1999); 7) Müller and Zähringer (1966); na, not analysed; 8) uncertain.

$$P_{21} = (3.52 \pm 0.30) \, P'_{21}[17.6(^{22}Ne/^{21}Ne)_c - 15.9]^{-1}, \quad (4)$$

where $P'_{21} = 1.63$ [Mg] + 0.6 [Al] + 0.32 [Si] + 0.22 [S] + 0.07 [Ca] + 0.021 [Fe+Ni].

The elemental concentrations are inserted in wt.%, and P_{21} results in units of $10^{-10}cm^3STP/g$ per Ma (Table 3).

4.2. CRE Ages

Published data permit some relevant assessments of exposure histories. The data for Norton County include two measurements by Kirsten et al. (1963) for an interior and an exterior sample for which ^{3}He$_c$ and ^{21}Ne$_c$ show differences of 7% and
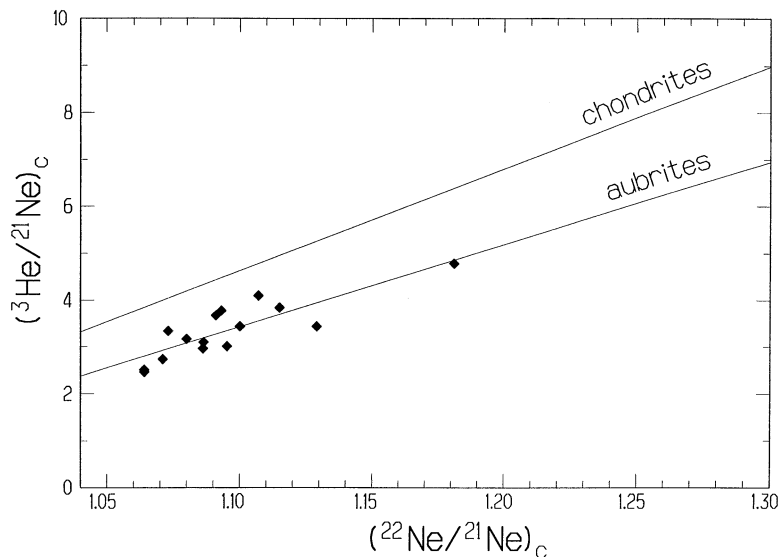

Fig. 3. 3He/^{21}Ne vs. ^{22}Ne/^{21}Ne diagram for Fe-poor (Fe $\leq$ 2%) aubrites. Aubres shows ^{3}He and ^{4}He loss and is not plotted.

Table 3. Production rates, P_i, CRE ages, T_i, $^{21}Ne_n$, and production rates $P(^{21}Ne_n)$.

	P_3	P_{21}	T_3	T_{21}	T_{81}	T_{pref}	$^{21}Ne_n$	$P(^{21}Ne_n)$
	$10^{-8}cm^3STP/g,Ma$				Ma		$10^{-8}cm^3STP/g$	$10^{-8}cm^3STP/g,Ma$
ALH 78113	1.755	0.522	20.3	22.0	–	21.1 ± 2.0	9.0	0.0180
ALH 84007	1.758	0.542	25.7	26.4	–	26.0 ± 2.5	11.4	0.0186
ALH 84011	1.755	0.523	30.6	23.3	–	22.0 ± 2.0	9.6	0.0185
ALH 84008	1.751	0.498	14.8	17.3	–	16.0 ± 1.6	6.6	0.0175
ALH 84024	1.767	0.571	13.6	15.4	–	14.5 ± 1.5	7.2	0.0210
Aubres	1.742	0.448	–	12.6	–	12.6 ± 2.0	4.2	0.0142
Bishopville	1.747	0.441	52.5	50.9	52[1] ± 5	52.0 ± 5.0	16.4	0.0147
Bustee	1.744	0.475	50.8	54.4	–	52.6 ± 5.0	19.4	0.0160
Cumberland Falls Fe-poor	1.756	0.510	–	56.8	45[1] ± 22	60.9 ± 6.0	22.8	0.0161
Cumberland Falls Fe-rich	1.634	0.377	–	64.9	–		19.4	0.0200
EET 90033	1.766	0.580	25.5	31.6	–	28.5 ± 3.0	15.4	0.0237
EET 90757	1.751	0.462	–	35.9	–	35.9 ± 5.0	12.2	0.0149
Khor Temiki	1.743	0.439	53.9	55.8	52[2] ± 17	53.9 ± 5.5	16.5	0.0134
LEW 87007	1.748	0.548	59.8	57.1	–	58.5 ± 6.0	25.6	0.0194
Mayo Belwa	1.738	0.407	102.4	127.4	117[1] ± 18	116 ± 12	35.1	0.0135
Mt. Egerton	1.628	0.387	10.0	26.9	–	26.9 ± 4.0	–	–
Norton County	1.749	0.523	117.4	104.2	–	111 ± 11	41.8	0.0151
Peña Blanca Springs	1.713	0.333	69.5	74.7	–	72.1 ± 7.0	13.6	0.0083
Pesyanoe light	1.756	0.543	50.0	36.3	–	43.2 ± 7.0	15.1	0.0135
Pesyanoe dark	1.759[4]	0.497[4]	–	24.5	–	24.5 ± 5.0	–	–
Pesyanoe-92 enstatite crystal 1	1.759	0.520	44.5	41.7	–		16.7	0.0195
Pesyanoe-92 enstatite crystal 2	1.759	0.474	44.0	43.7	–	43.5 ± 4.0	15.0	0.0142
Pesyanoe-90.2	1.759	0.520	48.0	63.2	–	55.6 ± 8.0	26.2	0.0195
QUE 97289	1.624[3]	0.446[3]	44.1	43.9	–	44.0 ± 4.5	17.1	0.0256
QUE 97348	1.624[3]	0.446[3]	–	37.2	–	37.2 ± 5.5	14.5	0.0256
Shallowater	1.628	0.280	27.0	27.1	–	27.0 ± 2.5	4.0	0.0075
Y 793592	1.759	0.554	48.5	61.4	–	55.0 ± 7.0	28.6	0.0243

1) Miura pers. comm. (2001); 2) Eugster et al. (1969); 3) the production rates were calculated with $(^{22}Ne/^{21}Ne)_c = 1.05$, as limit for P_3 and P_{21}; 4) average production rates of Pesyanoe-92 enstatite crystal 1 and 2 adopted.

11%, respectively, with higher interior production rates, consistent with the large recovered mass (~1000 kg), and shielding dependent production rates for 4π-irradiation. On the other hand, the cosmic ray-produced concentrations of $^{21}Ne_c$ in the light and dark phases of Pesyanoe (Müller and Zähringer, 1966) differ by almost a factor of 2 and are not consistent with shielding effects for 4π-irradiation of the rather small Pesyanoe meteorite. This is amplified by the ^{21}Ne data (Table 3) in Pesyanoe-90.2, also of the dark phase, which show a $^{21}Ne_c$ concentration that exceeds the one observed by Müller and Zähringer (1966) by more than a factor of 2. Furthermore, we have determined the spallation components in a single large enstatite and also in a collection of large crystals that yield consistent results (Tables 2, 3) and also agree with those of the light phase of Müller and Zähringer (1966). We discuss the implications regarding the irradiation history of Pesyanoe later.

The cosmic ray-produced noble gas abundances represent the integral production by cosmic rays and include all the components resulting from 2π-irradiation on the surface of the parent body. These effects need to be discussed individually, as they affect the exposure times in space (transfer times). We will first consider "nominal" calculated CRE ages, which are given in Table 3. ^3He exposure ages (T_3) are calculated using production rates from Eugster and Michel (1995); ^{21}Ne ages (T_{21}) are obtained using Eqn. 4 and concentrations given in Table 2. A "preferred nominal" CRE age (T_{pref}) is obtained as follows: (1) $T_{pref} = T_{81}$ is adopted if the errors in T_{81} are < 15%. (2) T_3 is not used for cases with possible ^3He losses, that is, for T_3

< 0.75 T_{21}. (3) If T_3 is included, $T_{pref} = 1/2 (T_3 + T_{21})$. We assign experimental uncertainties of 10% in case (3) and 15% in the other cases.

The nominal calculated CRE ages (Table 3; Fig. 4) show a non-uniform distribution, as was already observed by Eberhardt et al. (1965a) based on a limited dataset. A cluster of CRE ages of 56 ± 6 Ma includes Bishopville, Bustee, Cumberland Falls, Khor Temiki, Y 793592, and LEW 87007. However, some of these meteorites (Cumberland Falls, Khor Temiki, Mayo Belwa, and Shallowater) show neutron-capture effects, and the nominal CRE ages will be discussed with regard to possible regolith histories. The CRE ages of Norton County and Mayo Belwa are similarly long, the longest CRE ages of all stony meteorites. The ALH aubrites were found in the same location and for this reason were considered to represent a paired fall (Grady, 2000). However, their CRE ages differ: Two of these (ALH 84008 and ALH 84024) have CRE ages of 15 ± 2 Ma, while three (ALH 78113, ALH 84007, and ALH 84011) have ages of 23 ± 3 Ma. These data do not rule out possible pairing, but a model of regolith evolution and precompaction irradiation would be necessary to explain the data. We note that two members with ages ~23 Ma also reveal small positive $\Delta^{17}O$ excesses (Newton et al., 2000), indicating the possible presence of non-aubritic material in these breccias. The CRE age distribution shows that there are no young (< 10 Ma) ages. Thus, the orbital characteristics of enstatite chondrites differ from those of aubrites, as suggested previously by Gaffey et al. (1992).
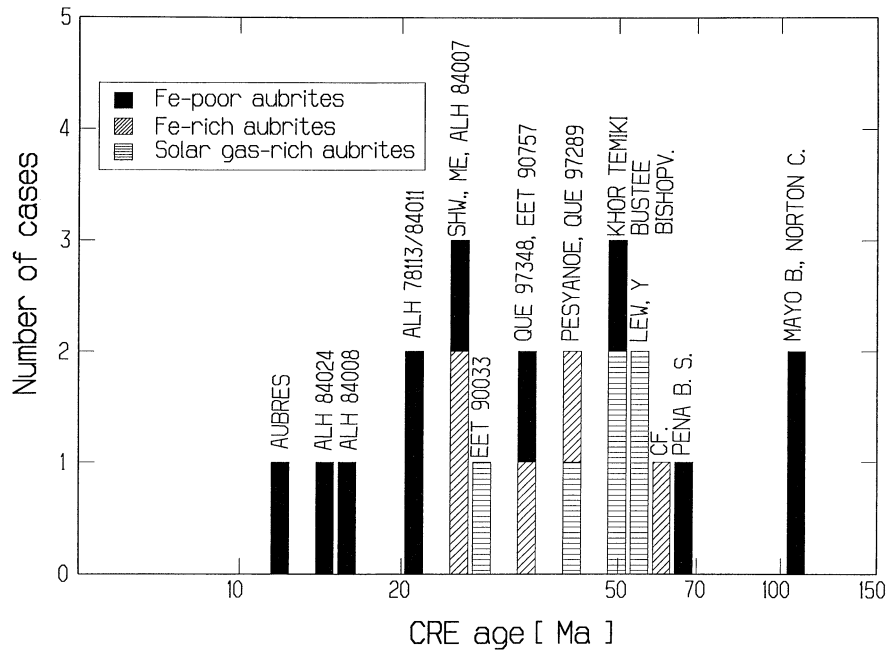
Fig. 4. CRE age histogram for aubrites. The CRE age of each aubrite was arranged to 10% age bins. The first bin contains ages between 1 and 1.1 Ma. The Pesyanoe data document the light phase and the enstatite separates.

4.3. Neutron-Induced Excesses in Ne and Kr

The depth-dependent ratio of neutron-induced (n) ^{21}Ne to total ^{21}Ne$_c$ was determined by Michel et al. (1991) for several meteorites with known geometry. The concentrations of ^{21}Ne$_n$ are calculated following Eugster et al. (1993):

$$^{21}Ne_n = {}^{21}Ne_c [3.5 - 2.5({}^{22}Ne/{}^{21}Ne)_c], \qquad (5)$$

and results are listed in Table 3.

Cumberland Falls, Khor Temiki, Mayo Belwa, and Shallowater indicate neutron-capture-produced components of ^{80}Kr and ^{82}Kr (Figs. 5a,b). The concentrations of ^{80}Kr$_n$ and ^{82}Kr$_n$ (Table 1) are calculated by subtracting pure spallation (s) contributions based on $(^{80}Kr/^{83}Kr)_s = 0.560 \pm 0.036$ and $(^{82}Kr/^{83}Kr)_s = 0.764 \pm 0.023$. These spallation ratios were obtained by (1) adopting Kr data to represent mixtures of spallation and trapped components (for those lacking neutron effects) and by extrapolating isotopic correlations to the spallation endmember ratio $(^{86}Kr/^{83}Kr)_s = 0.015$; and (2) by subtraction of the adopted trapped component based on ^{86}Kr$_{tr}$. The estimated errors include the uncertainties of spallation and trapped datasets. Subtraction of the trapped and cosmogenic concentrations from measured data yields the concentrations of ^{80}Kr$_n$ and ^{82}Kr$_n$ (Table 1). The $(^{80}Kr/^{82}Kr)_n$ ratios are 2.8 ± 0.7 and 1.9 ± 1.5 for Cumberland Falls and Shallowater, respectively, and the $(^{80}Kr/^{128}Xe)_n$ ratio in Cumberland Falls is 10.9 ± 2.5. Marti et al. (1966) deduced values in the ranges 1.6 to 3.5 for $(^{80}Kr/^{82}Kr)_n$ and 12.4 to 42.0 for $(^{80}Kr/^{128}Xe)_n$, depending on the hardness of the neutron energies. The $(^{80}Kr/^{82}Kr)_n$ ratios reflect neutron fluences of epithermal energies (30–300 eV), the resonance region for neutron capture of Br (Marti et al., 1966).

4.4. Preirradiation Effects

Above we discussed evidence for preirradiation effects in the regolith on the parent body. Several types of monitors of regolith exposure are known and may be used to study regolith histories of meteorites: (a) the occurrence of clasts of distinct composition in brecciated host material; (b) evidence for SW loading; (c) evidence for neutron-capture effects; (d) discrepancies of CRE ages of components in a breccia; (e) identification of fission components due to neutron-induced fission of ^{235}U. These records have successfully been used in studies of the lunar regolith (Lingenfelter et al., 1972) and in a similar manner may be used to assess processes in asteroidal regoliths. Clear cases of complexity can be inferred if regolith evolution from several monitors is observed. The Cumberland Falls meteorite exhibits evidence for the occurrence of clasts of chondritic composition (Mason, 1962). This meteorite was classified as an outlier sample in the O isotopic data (Clayton et al., 1984; Newton et al., 2000). It also shows evidence for large neutron fluences in the form of Sm and Gd isotopic shifts (Hidaka et al., 1999). Large neutron-capture effects in Sm and Gd isotopic abundances were also observed by these authors in four aubrites: Norton County, ALH 78113, Bishopville, and Mayo Belwa. Although small neutron capture effects have to be expected for very long space exposure times, the implied neutron flux is very large in the case of Cumberland Falls. Hidaka et al. (1999) suggested that variable neutron fluences may be expected for near-surface locations on their parent body. A comparison of neutron effects with other regolith monitors is useful.

The following aubrites were listed as regolith breccias by Newton et al. (2000): Bustee, Khor Temiki, and Pesyanoe. These three aubrites contain solar-type gases. This is also the
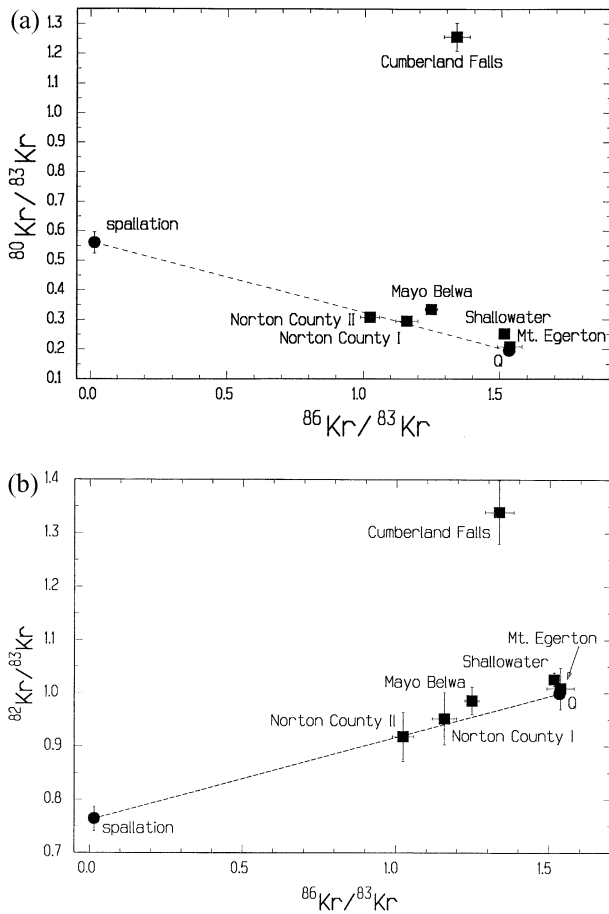
Fig. 5. (a) ^{80}Kr/^{83}Kr and ^{86}Kr/^{83}Kr ratios as measured in aubrites. Cumberland Falls, Khor Temiki, Mayo Belwa, and Shallowater contain ^{80}Kr$_n$ components in addition to spallation Kr. (b) ^{82}Kr/^{83}Kr and ^{86}Kr/^{83}Kr ratios as measured in aubrites. Cumberland Falls, Mayo Belwa, Khor Temiki, and Shallowater contain ^{82}Kr$_n$ components.

case for EET 90033, LEW 87007, and Y 793592, which may also be classified as regolith breccias. Support for this classification is obtained from petrographic properties, such as light-dark structure and inclusions of different composition in a brecciated host. We do not find evidence in aubrites for impact-melt spherules such as those found in howardites and lunar breccias (Bunch, 1975). Not all aubrites with foreign clasts are solar gas carriers; Cumberland Falls is such an exception (Table A4). Most aubrites are brecciated, but only Shallowater was considered to have an impact origin (Keil et al., 1989).

It is informative to compare cosmic ray effects due to fast (> 5 MeV) neutrons (^{21}Ne$_n$) to those resulting from epithermal neutrons (^{80}Kr$_n$) and thermal neutrons (^{157}Gd) (Hidaka et al., 2000). ^{80}Kr$_n$ excesses were observed in the four aubrites, Cumberland Falls, Khor Temiki, Mayo Belwa, and Shallowater (Table 3), and thermal neutron effects were reported in two of these (Hidaka et al., 1999). Neutron fluxes, ϕ_n, for neutrons with energies > 5 MeV, as required for the reaction ^{24}Mg (n, α) ^{21}Ne, are obtained from:

$$\phi_n = P(^{21}Ne_n)/\sigma, \qquad (6)$$

where P'(^{21}Ne$_n$) is the ^{21}Ne$_n$ atomic production rate per target

atom and $\sigma = 0.0562 \times 10^{-24}$cm^2 (Michel, 1991, pers. comm.), the capture cross section for ^{24}Mg. The neutron flux ϕ_n results in neutrons/cm^2 per second, if P'(^{21}Ne$_n$) is inserted in ^{21}Ne$_n$ atoms/^{24}Mg atoms per second. P'(^{21}Ne$_n$) in these dimensions is calculated from

$$P(^{21}Ne_n) = 4.38 \times 10^{-23} P(^{21}Ne_n), \qquad (7)$$

where P'(^{21}Ne$_n$) is obtained from ^{21}Ne$_n$ and T$_{pref}$ in Table 3 and from Mg in Table A4:

$$P(^{21}Ne_n) = \frac{^{21}Ne_n}{Mg \times T_{pref.}} \qquad (8)$$

P(^{21}Ne$_n$), given in Table 3, has the dimension 10^{-8}cm^{3}STP/g per wt.% and Ma. Thus, we use:

$$\phi_n = 779 \ P(^{21}Ne_n). \qquad (9)$$

The resulting (fast) neutron fluxes ϕ_n(Ne) are given in Table 4.

High ϕ_n (Ne) values are obtained for the aubrites EET 990033, LEW 87007, and Y 793592, which also contain SW gas components and, therefore, reveal an evolution in a regolith.

The abundant SW-Ne component in the dark phase of Pesyanoe precludes the evaluation of the spallation Ne ratio. However, the (^{22}Ne/^{21}Ne)$_c$ ratios, as well as CRE ages of the light phase and of the separated enstatite crystals of the dark phase (Table 3), agree well with each other and permit the use of approximately constant production rates P$_{21}$ for Pesyanoe dark and Pesyanoe light. As indicated earlier, the calculated irradiation times (T$_{21}$) for these two phases (Table 3) differ considerably; this discrepancy documents a preirradiation of components in the regolith before compaction of the Pesyanoe aubrite. Furthermore, T$_{21}$ of the Pesyanoe (dark) sample 90-2, is higher than all the other Ne ages measured in Pesyanoe. A complex regolith history is also evident by the identification of a fractionated solar component, elementally and isotopically fractionated solar-type gas (Mathew and Marti, 2002, pers. comm.), and by large neutron-capture effects in Gd and Sm (Table 1). To infer actual effective neutron fluences, the ^{80}Kr$_n$ excesses (Table 1) need to be normalized to Br abundances in aliquot samples, as the Br abundance is quite variable in aubrites. Because no Br data are presently available, the neutron fluxes cannot be calculated.

Hidaka et al. (1999) compared the neutron fluences inferred from Sm of aubrites with those observed on the lunar surface. These neutron fluences are of the same magnitude. However, the neutron slowing-down densities may differ, since the effective capture cross sections are affected by strong resonance capture on the moon (Lingenfelter et al., 1972) and because of possible differences in the CR intensity and temperature on the aubrite parent object at the time of irradiation. Using an intensity of cosmic radiation corresponding to that at solar minimum in the polar region of the Earth (8.4 n cm^{-2}s^{-1}) given by Lingenfelter et al. (1972), a dependence of neutron production on the average atomic mass of aubrites, and the procedure used by these authors to estimate the contributions by π-mesons and leakage losses, we estimate a production rate of 17 n cm^{-2}s^{-1} for neutrons (E < 10 MeV) and an attenuation length of 165 g cm^{-2}. Lingenfelter et al. (1972) pointed out that higher temperatures shift the flux spectrum to higher energies. The capture

Table 4. Characterization of the aubrites.

	Brecciation	Inclusions	>10 vol % metallic iron	Shock blackening	Solar ^{36}Ar[3]	^{80}Kr$_n$[4]	ϕ_n(Ne) n cm^{-2}s^{-1}	ϕ_n (Sm)[5] (n cm^{-2}s^{-1})	CRE age (Ma)
ALH 78113	yes	chondritic	no	1)	0	–	14.0	21.8	21.2
ALH 84007	yes	none	no	1)	0	–	14.5	–	26.0
ALH 84011	yes	none	no	1)	0	–	14.4	–	22.0
ALH 84008	yes	none	no	1)	0	–	13.6	–	16.0
ALH 84024	yes	none	no	1)	0	–	16.4	–	14.5
Aubres	yes	none	no	no	0	–	11.1	–	12.6
Bishopville	yes	none	no	no	0	–	11.4	19.6	52.0
Bustee	yes	none	no	no	3.5	–	12.5	–	52.6
Cumberland Falls	yes	chondritic	no	no	0	15.3	14.1	41.0	60.9
EET 90033/90757	yes	none	no	2)	1.4	–	15.0	–	32.2
Khor Temiki (3μm)	yes	none	no	no	19.3	0.52	10.5	–	53.9
LEW 87007	yes	none	no	2)	10.8	–	15.1	–	58.5
Mayo Belwa	yes	none	no	yes	0	1.5	10.5	7.4	117
Mt. Egerton	no	none	yes	no	0	< 0.4	–	–	26.9
Norton County	yes	none	no	no	0	< 0.4	11.7	4.7	111
Pena Blanca Springs	yes	none	no	no	0	–	6.5	–	72.1
Pesyanoe light	yes	chondritic ?	no	no	0.3	–	10.6	–	43.2
Pesyanoe dark	yes	chondritic ?	no	no	271	–	–	23.8	47
QUE 97289/97348	no	none	yes	no	0	–	20.0	–	40.6
Shallowater	no	chondritic	yes	no	0	10.5	5.9	–	27.0
Y 793592	yes	none	no	yes ?	3.9	–	18.9	–	55.0

1) Some ALH samples appear shock-blackened and some do not. We do not have the specific samples to determine if these samples are shock-blackened. 2) EET 90033, EET 90757, and LEW 87007 are too small to determine shock-blackening. 3) In 10^{-8}cm^3 STP/g. 4) In 10^{-12}cm^3 STP/g. 5) Calculated from Sm data of Hidaka et al. (1999) and Hidaka, priv. comm. (2001).

rates with the lowest resonances (e.g., ^{157}Gd) decrease, those with slightly higher energy (e.g., ^{149}Sm) increase, while epithermal resonances are little affected (e.g., ^{79}Br). Such systematics may be useful in assessing preirradiation conditions.

To disentangle 2π-irradiation effects from space exposure in 4π-geometry and to assess neutron capture systematics, we may take advantage of the large preatmospheric size of Norton County and of its long CRE age of 111 ± 11 Ma (Table 3) as a potential standard for 4π-irradiation. In this model the CRE age of Norton County represents the space exposure time. Regarding neutron effects in Norton County, we obtain an upper limit for ^{80}Kr$_n$ of 0.4 × 10^{-12}cm^{3}STP/g (Table 1), an integral neutron capture rate in ^{157}Gd per initial ^{157}Gd atom of 14.1 × 10^{-4}, and in ^{149}Sm per initial ^{149}Sm atom a capture rate of 6.8 × 10^{-4}. The ratio Δ^{157}Gd/Δ^{149}Sm = 2.07 is smaller than the cross-section ratio for thermalized neutrons ($\sigma_{157}/\sigma_{149}$ = 5.8), indicating that the neutron spectrum was not thermalized. The observed ^{149}Sm loss by neutron capture requires an average neutron flux of 4.6 n cm^{-2}s^{-1} during the CRE age (using σ_{149} = 4.2 × 10^4 barn), which happens to be consistent, within uncertainties, with the flux inferred for the Abee enstatite chondrite (Hidaka et al., 1999). All other Sm data reported for aubrites suggest larger neutron fluxes, if the Gd and Sm anomalies were assigned to 4π-irradiation times corresponding to the CRE data in Table 3. For example, the neutron flux inferred for the Cumberland Falls aubrite, based on a CRE age of 60.9 ± 6.0 Ma (Table 3) yields 40 n cm^{-2}s^{-1}, which far exceeds the earlier given neutron production rate (E < 10 MeV). Cumberland Falls clearly indicates a regolith history. This evidence is consistent with our results from Kr$_n$ data and with the presence of inclusions.

The neutron flux inferred for Bishopville, another member of the 56 ± 6 Ma cluster, is 20 n cm^{-2} s^{-1}, also exceeding the neutron production rate. In both cases the neutron exposure time must have been considerably longer than the time indicated by the CRE age. Hidaka et al. (1999) estimated irradiation time intervals for aubrites of several 10^8 years, as typically inferred for the lunar regolith. These preirradiation time intervals invalidate the use of nominal (4π-geometry) CRE ages, since a significant fraction of the spallation component was produced during the regolith history. Therefore, the existence of a CRE age cluster at 56 ± 6 Ma becomes questionable. There is also evidence for a ^{80}Kr excess due to neutron irradiation in Khor Temiki (Table 3), another member of this "cluster." And there is evidence for solar-type noble gases in Khor Temiki, Y 793592, and LEW 87007 (Table 5), which requires a regolith history for these aubrites before compaction into the present meteorites. We have presented evidence for regolith evolution for all six members of this cluster. The CRE ages observed by Eberhardt et al. (1965a) are calculated from the sum of the noble gases produced during the transfer time and the preejection exposure on the parent body.

Therefore, a single collisional event, which is usually implied to account for consistent CRE ages, appears doubtful. Regolith revolution affects generally the spallation data of meteorites in a different fashion.

5. CONCLUSIONS

We report nominal CRE ages for nine aubrites and reassess an earlier suggestion that a cluster appears in the CRE histogram. The new data confirm a non-uniform distribution of exposure times but undermine the significance of clusters in terms of collisional events, since many aubrites apparently were preirradiated in a parent body regolith. About one-third of all aubrites reveal the presence of solar wind (SW) gases, some show very large neutron-capture anomalies, and some have inclusions of non-aubritic composition. Table 4 presents infor-

Table 5. Trapped solar noble gases in aubrites.

	^{4}He	^{20}Ne	^{36}Ar	^{84}Kr	^{132}Xe	
			10^{-8}cm^{3}STP/g			Ref.
Bustee	5'800	120	3.5	–	–	1)
EET 90033	–	27	1.4	–	–	2)
Khor Temiki 3 μm fraction	289'000	786	19.3	–	–	3)
Khor Temiki	–	–	–	0.0044	0.00088	4)
LEW 87007	148'400	384	10.8	–	–	2)
Pesyanoe dark	1'066'000	3'600	271	–	–	5)
Pesyanoe (A)	1'040'000	2'680	163	0.072	0.0096	6)
Pesyanoe–90.2	852'000	4'260	148	–	–	2)
Y 793592	6'560	137	3.9	–	–	2)

References: 1) Poupeau et al. (1974); 2) this work; 3) Eberhardt et al. (1966); 4) Eugster et al. (1969); 5) Müller and Zähringer (1966); 6) Marti (1969).

mation on brecciation, foreign inclusions, neutron effects, and SW components, which represent the markers of a regolith breccia. The results confirm earlier reports of very long CRE ages and indicate orbital elements for its parent body that are distinct from those of enstatite chondrites. On the other hand, the actual transfer times may be substantially shorter in cases where the preirradiation in the regolith accounts for a significant fraction of the integral exposure time.

Associate editor: G. Herzog

REFERENCES

Anders E. and Grevesse N. (1989) Abundances of the elements: Meteoritic and solar. *Geochim. Cosmochim. Acta* **53**, 197–214.

Begemann F., Geiss J., and Hess D. C. (1957) Radiation age of a meteorite from cosmic-ray-produced ^{3}He and ^{3}H. *Phys. Rev.* **107**, 540–542.

Benkert J. P., Baur H., Signer P., and Wieler R. (1993) He, Ne, and Ar from the solar wind and solar energetic particles in lunar ilmenites and pyroxenes. *J. Geophys. Res.* **98**, 13147–13162.

Binns R. A. (1969) A chondritic inclusion of unique type in the Cumberland Falls meteorite. In *Meteorite Research* (ed. P. M. Millman), pp. 696–704, D. Reidel, Dordrecht.

Biswas S., Walsh T., Bart G., and Lipschutz M. E. (1980) Thermal metamorphism of primitive meteorites-XI. The enstatite meteorites: Origin and evolution of a parent body. *Geochim. Cosmochim. Acta* **44**, 2097–2110.

Bogard D. D., Nyquist L. E., Bansal B. M., Garrison D. H., Wiesmann H., Herzog G. F., Albrecht A. A., Vogt S., and Klein J. (1995) Neutron-capture ^{36}Cl, ^{41}Ca, ^{36}Ar, and ^{150}Sm in large chondrites: Evidence for high fluences of thermalized neutrons. *J. Gephys. Res.* **100**, 949–9416.

Bunch T. E. (1975) Petrography and petrology of basaltic achondrite polymict breccias (howardites). *Proc. Lunar Sci. Conf.* **6**, 469–492.

Burbine T. H., McCoy T. J., and Dickinson T. L. (2000) Origin of plagioclase-"enriched," igneous, enstatite meteorites (abstract). *Meteorit. Planet. Sci.* **35**, A36.

Burger M., Eugster O., and Krähenbühl U. (1989) Refractory trace elements in different classes of achondrites by RNAA and INAA and some noble gas data (abstract). *Meteoritics* 24:256–257.

Busemann H., and Eugster O. (2002) The trapped noble gas component in achondrites. *Meteorit. Planet. Sci.* (in press).

Busemann H., Baur H., and Wieler R. (2000) Primordial noble gases in "Phase Q" in carbonaceous and ordinary chondrites studied by closed system stepped etching. *Meteorit. Planet. Sci.* **35**, 949–973.

Casanova I., McCoy T. J., and Keil K. (1993) Metal-rich meteorites from the aubrite parent body (abstract). *Lunar Planet. Sci.* 24:259–260.

Clayton R. N., Mayeda T. K., and Rubin A. E. (1984) Oxygen isotopic composition of enstatite chondrites and aubrites. *Proc. Lunar Planet. Sci. Conf.* **15**, C245–C249.

Crabb J. and Anders E. (1981) Noble gases in E-chondrites. *Geochim. Cosmochim. Acta* **45**, 2443–2464.

De Laeter J. R. and Hosie D. J. (1978) The abundance of barium in stony meteorites. *Earth Planet. Sci. Lett.* **38**, 416–420.

Djakonowa M. J. and Charitonowa W. J. (1960) Results on chemical analyses of meteorites collected in the Sowjet Union. *Meteoritica* **18**, 48–67.

Easton A. J. (1985) Seven new bulk chemical analyses of aubrites. *Meteoritics* **20**, 571–573.

Eberhardt P., Eugster O., and Geiss J. (1965a) Radiation ages of aubrites. *J. Geophys. Res.* **70**, 4427–4434.

Eberhardt P., Eugster O., and Marti K. (1956) A redetermination of the isotopic compositions and atmospheric wear meteoritica, **20a**, 623.

Eberhardt P., Geiss J., and Grögler N. (1965c) Über die Verteilung der Uredelgase im Meteoriten Khor Temiki. *Tscher. Mineral. Petrog.* **10**, 535–551.

Eberhardt P., Geiss J., and Grögler N. (1966) Distribution of rare gases in the pyroxene and feldspat of the Khor Temiki meteorite. *Earth Planet. Sci. Lett.* **1**, 7–12.

Ehmann W. D. and Rebagay T. V. (1970) Zirconium and hafnium in meteorites by activation analysis. *Geochim. Cosmochim. Acta* **34**, 649–658.

Eugster O. (1967) Isotopenanalysen von Krypton und Xenon in Steinmeteoriten und ihre Deutung. Ph.D. thesis, Univ. of Bern.

Eugster O. (1988) Cosmic-ray production rates for ^{3}He, ^{21}Ne, ^{38}Ar, ^{83}Kr, and ^{126}Xe in chondrites based on ^{81}Kr-Kr exposure ages. *Geochim. Cosmochim. Acta* **52**, 1649–1662.

Eugster O. and Michel T. (1995) Common asteroid break-up events of eucrites, diogenites, and howardites and cosmic-ray production rates for noble gases in achondrites. *Geochim. Cosmochim. Acta* **59**, 177–199.

Eugster O., Eberhardt P., and Geiss J. (1969) Isotopic analyses of krypton and xenon in fourteen stone meteorites. *J. Geophys. Res.* **74**, 3874–3896.

Eugster O., Michel T., Niedermann S., Wang D., and Yi W. (1993) The record of cosmogenic, radiogenic, fissiogenic, and trapped noble gases in recently recovered Chinese and other chondrites. *Geochim. Cosmochim. Acta* **57**, 1115–1142.

Eugster O., Terribilini D., Polnau E., and Kramers J. (2001) The antiquity indicator argon-40/argon-36 for lunar surface samples calibrated by uranium-235-xenon-136 dating. *Meteorit. Planet. Sci.* **36**, 1097–1116.

Gaffey M. J., Reed K. L., and Kelley M. S. (1992) Relationship of E-type Apollo Asteroid 3103 (1982 BB) to the aubrite meteorites and the Hungaria Asteroids. *Icarus* **100**, 95–109.

Grady M. M. (2000) *Catalogue of Meteorites.* Cambridge University Press, Cambridge, England.

Graf T., and Marti K. (1992) Cosmic-ray exposure history of enstatite chondrites. (abstract). *Meteoritics* **27**, 227.

Graham A. L. and Henderson P. (1985) Rare earth element abundances in separated phases of Mayo Belwa, an enstatite chondrite. *Meteoritics* **20**, 141–149.

Herpers U., Vogt S., Bremer K., Hofmann H. J., Suter M., Wieler R., Lange H.-J., and Michel R. (1995) Cosmogenic nuclides in differentiated Antarctic meteorites: Measurements and model calculations. *Planet. Space Sci.* **43**, 545–556.

Herzog G. F., Cressy P. J., and Carver E. A. (1977) Shielding effects in Norton County and other aubrites. *J. Geophys. Res.* **82**, 3430–3436.

Heusser G., Hampel W., Kirsten T., and Schaeffer O. A. (1978) Cosmogenic isotopes in recently fallen meteorites (abstract). *Meteoritics* **13**, 492–494.

Hidaka H., Ebihara M., and Yoneda S. (1999) High fluences of neutrons determined from Sm and Gd isotopic compositions in aubrites. *Earth Planet. Sci. Lett.* **173**, 41–51.

Hidaka H., Ebihara M., and Yoneda S. (2000) Isotopic study of neutron capture effects on Sm and Gd in chondrites. *Earth Planet. Sci. Lett.* **180**, 29–37.

Ivanova M. A., Burbine T. H., Dickinson T. L., and McCoy T. J. (2002) An FeO-rich clast from the Pesyanoe aubrite. Indigenous or foreign? *Lunar Planet. Sci. XXXIII*, abstract #1080, Lunar Planet. Inst., Houston, CD-ROM.

Jarosewich E. (1967) Chemical analyses of seven stony meteorites and one iron with silicate inclusions. *Geochim. Cosmochim. Acta* **31**, 1103–1106.

Kallemeyn G. W. and Wasson J. T. (1985) The compositional classification of chondrites: IV. Ungrouped chondritic meteorites and clasts. *Geochim. Cosmochim. Acta* **49**, 261–270.

Keil K. (1968) Mineralogical and chemical relationships among enstatite chondrites. *J. Geophys. Res.* **73**, 6945–6976.

Keil K., Ntaflos T., Taylor G. J., Brearley A. J., Newsom H. E., and Romig A. D. Jr (1989) The Shallowater aubrite: Evidence for origin by planetesimal impact. *Geochim. Cosmochim. Acta* **53**, 3291–3307.

Kirsten T., Krankowsky D., and Zähringer J. (1963) Edelgas- und Kalium-Bestimmungen an einer grösseren Zahl von Steinmeteoriten. *Geochim. Cosmochim. Acta* **27**, 13–42.

Laul J. C., Keays R. R., Ganapathy R., Anders E., and Morgan J. W. (1972) Chemical fractionation in meteorites-V. Volatile and siderophile elements in achondrites and ocean ridge basalts. *Geochim. Cosmochim. Acta* **36**, 329–345.

Levsky L. K. (1972) New Data on the isotopic composition of meteorites. *Meteoritica* **31**, 149–150.

Lingenfelter R. E., Canfield E. H., and Hampel V. E. (1972) The lunar neutron flux revisited. *Earth Planet. Sci. Lett.* **16**, 355–369.

Lipschutz M. E., Verkouteren R. M., Sears D. W. G., Hasan F. A., Prinz M., Weisberg M. K., Nehru C. E., Delaney J. S., Grossman L., and Boily M. (1988) Cumberland Falls chondritic inclusions: III. Consortium study of relationship to inclusions in Allan Hills 78113 aubrite. *Geochim. Cosmochim. Acta* **52**, 1835–1848.

Lodders K., Palme H., and Wlotzka F. (1993) Trace elements in mineral separates of the Peña Blanca Spring aubrite: Implications for the evolution of the aubrite parent body. *Meteoritics* **28**, 538–551.

Lonsdale J. T. (1947) The Pena Blanca Spring meteorite, Brewster County, Texas. *Am. Mineral.* **32**, 354–364.

Lorenzetti S., Eugster O. (2000) Break-up history of the enstatite achondrite. (aubrite) parent asteroid. *Lunar Planet. Sci. XXXI*, abstract #1017, Lunar Planet. Inst., Houston, CD-ROM.

Lorenzetti S., Eugster O., Burbine T., McCoy T., and Marti K. (2001) Break-up events on the aubrite parent body. *Meteorit. Planet. Sci.* **36**, A116–A117.

Marti K. (1969) Solar-type xenon: A new isotopic composition of xenon in the Pesyanoe meteorite. *Science* **166**, 1263–1265.

Marti K., Eberhardt P., and Geiss J. (1966) Spallation, fission, and neutron capture anomalies in meteoritic kryton and xenon. *Z. Naturforsch.* **21a**, 398–413.

Mason B. (1962) Meteorites. John Wiley and Sons Inc., New York.

Mason B. (1978) Meteorites. In *Data of Geochemistry.* (ed. M. Fleischer); 6th ed., Chap. B, Cosmochemistry, Part 1, 118.

Mathew K. J. and Marti K. (2001) Lunar nitrogen: Indigenous signature and cosmic ray production rate. *Earth Planet. Sci. Lett.* **184**, 659–669.

McCoy T. J., Keil K., Bogard D. D., Garrison D. H., Casanova I., Lindstrom M. M., Brearley A. J., Kehm K., Nichols R. H. Jr., and Hohenberg C.M. (1995) Origin and history of impact-melt rocks of enstatite chondrite parentage. *Geochim. Cosmochim. Acta* **59**, 161–175.

Mewald R. A., Ogliore R. C., Gloeckler G., and Mason G. M. (2001) A new look at solar Neon-C and SEP-Neon. CP 598. (ed. R. R. Wimmer-Schweingruber), American Institute of Physics, 393–398.

Michel R., Dragovitsch P., Cloth P., Dagge G., and Filges D. (1991) On the production of cosmogenic nuclides in meteoroids by galactic protons. *Meteoritics* **26**, 221–242.

Miura Y. N., Nagao K., and Okazaki R. (1999) *Noble gases in five aubrites, Cumberland Falls, Mayo Belwa, Mt. Egerton, Norton County, and Pena Blanca Spring. Antarctic Meteorites XXIV*, pp.108–110. Natl. Inst. Polar Res., Tokyo.

Müller O. and Zähringer J. (1966) Chemische Unterschiede bei uredelgashaltigen Steinmeteoriten. *Earth Planet. Sci. Lett.* **1**, 25–29.

Müller H. W. and Zähringer J. (1969) Rare gases in stony meteorites. In *Meteorite Research* (ed. P. M. Millman), pp. 845–856. D. Reidel, Dordrecht.

Murty S. V. S. and Marti K. (1990) Search for solar type nitrogen in the gas-rich Pesyanoe meteorite. *Meteoritics* **25**, 227–230.

Neal C. W. and Lipschutz M. E. (1981) Cumberland Falls chondritic inclusions: Mineralogy/petrology of a forsterite chondrite suite. *Geochim. Cosmochim. Acta* **45**, 2091–2107.

Newton J., Franchi I. A., and Pillinger C. T. (2000) The oxygen isotopic record in enstatite meteorites. *Meteorit. Planet. Sci.* **35**, 689–698.

Okada A., Keil K., Taylor G. J., and Newsom H. (1988) Igneous history of the aubrite parent asteroid: Evidence from the Norton County aubrite. *Meteoritics* **23**, 59–74.

Patzer A. and Schultz L. (2001) Noble gases in enstatite chondrites I: Exposure ages, pairing, and weathering effects. *Meteorit. Planet. Sci.* **36**, 947–961.

Poupeau G., Kirsten T., Steinbrunn F., and Störzer D. (1974) The records of solar wind and solar flares in aubrites. *Earth Planet. Sci. Lett.* **24**, 229–241.

Schultz L. and Franke L. (2000) *Helium, neon and argon in meteorites, a data compilation.* Max-Planck-Institute for Chemistry, Mainz.

Shimizu H. and Masuda A. (1981) REE, Ba, Sr and Rb abundances in some unique antarctic achondrites (abstract). *Proc. NIPR Symp. Antarct. Meteorites* **6**, 211–220.

Vogt S., Herpers U., Sarafin R., Signer P., Wieler R., Suter M., and Wölfli W. (1986) *Cosmic ray records in antarctic meteorites - A data compilation of the Cologne-Zürich-collaboration. Workshop on Antarctic Meteorites, LPI Techn. Report*, pp. 86–01. The Lunar Planet. Inst., Houston.

Von Michaelis H., Ahrens L. H., and Willis J. P. (1969) The composition of stony meteorites II. The analytical data and an assessment of their quality. *Earth Planet. Sci. Lett.* **5**, 387–394.

Wacker J. F. (1982) Composition of noble gases in the Abee meteorite and the origin of enstatite chondrites. Ph.D. thesis, Univ. of Arizona.

Wasson J. T. and Wai C. M. (1970) Composition of metal, schreibersite and perryite of aubrites and the origin of enstatite chondrites and achondrites. *Geochim. Cosmochim. Acta* **31**, 169–184.

Watters T. R. and Prinz M. (1979) Aubrites: Their origin and relationship to enstatite chondrites. *Proc. Lunar Planet. Sci. Conf.* **10**, 1073–1093.

Wiik H. B. (1956) The chemical composition of some stony meteorites. *Geochim. Cosmochim. Acta* **9**, 279–289.

Wolf R., Ebihara M., Richter G. R., and Anders E. (1983) Aubrites and diogenites: Trace element clues to their origin. *Geochim. Cosmochim. Acta* **47**, 2257–2270.

Yanai K. (1992) Yamato-793592: The first aubrite (aubrite) in the Yamato meteorite collections. *Proc. NIPR Symp. Antarct. Meteorites.* **5**, 235–241.

Zähringer J. (1968) Rare gases in stony meteorites. *Geochim. Cosmochim. Acta* **32**, 209–237.

Table A1. Chemical composition of aubrites (concentrations in wt. %).

	Na	Mg	Al	Si	K	Ca	Ti	Cr	Mn	Fe	Ni	References
ALH aubrites	0.073	23.6	0.16	27.1	0.012	0.46	0.027	0.037	0.13	0.48	0.030	1), 2), 3)
Aubres	0.071	23.4	0.18	27.6	0.052	0.38	0.069	0.027	0.10	0.65	0.034	4), 5)
Bishopville	0.54	21.5	1.09	27.4	0.108	0.92	0.020	0.018	0.030	0.62	0.026	4), 5)
Bustee	0.23	23.0	0.25	26.8	0.014	1.44	0.030	0.026	0.12	0.82	0.018	4), 5)
LEW 87007	0.26	22.6	0.90	27.0	0.05	1.00	0.05	0.02	0.17	0.06		1)
EET aubrites	0.18	22.8	0.26	27.4	0.045	1.02	0.045	0.025	0.10	0.13		1)
Khor Temiki	0.29	22.8	0.50	27.6	0.048	0.47	0.024	0.026	0.05	0.95	0.04	4), 5)
Mayo Belwa	0.95	22.2	0.66	27.8	0.067	0.40	0.035	0.031	0.09	0.33	0.01	4), 5)
Mt. Egerton	0.01	19.0	0.08	23.0		0.25	0.01	0.01	0.03	19.0	1.20	13)
Norton County	0.17	25.0	0.14	25.3	0.012	0.85	0.029	0.032	0.11	1.22	0.027	4), 5), 6), 7)
Pena Blanca Spring	0.28	22.7	0.42	27.2	0.022	0.77	0.042	0.047	0.13	0.49	0.006	4), 5), 6), 8)
Y 793592	0.71	21.4	1.16	26.4	0.091	1.23	<0.01	0.017	0.014	0.7	0.32	2)
QUE aubrites	0.56	15.2	1.07	19.8	0.03	0.39	0.17	0.21	0.01	23.0	1.71	1)
Shallowater	0.32	19.7	0.40	23.0	0.026	0.13	0.012	0.027	0.068	13.5	0.73	4), 5)
Pesyanoe (average)	0.12	22.6	0.76	27.3	0.033	0.67	0.033	0.028	0.072	0.56	0.35	4), 10)
(dark)		22.5	0.8	27.0	0.065	0.8	0.04	0.06	0.16	1.2	0.002	9)
(light)		25.8	0.04	27.1	0.003	0.34	0.02	0.01	0.07	0.2	0.002	9)
Pesyanoe (enstatite)	0.015	24.2	0.048	27.8		0.32	0.018	0.02	0.023	0.047		4)
Cumberland Falls (av.)	0.4	23.2	0.11	26.7	0.011	0.45	0.012	0.094	0.062	2.65	0.06	4), 6)
(Fe-rich incl.)	0.93	15.9	1.37	19.7	0.091	1.38	0.093	0.31	0.50	19.25	1.00	11), 12)
Average for Fe-poor (Fe <2%) aubrites												
	0.34	22.8	0.52	27.1	0.047	0.81	0.034	0.028	0.095	0.59	0.046	1)

1) This work
2) Yanai (1992)
3) Herpers et al. (1995)
4) Watters and Prinz (1979)
5) Easton (1985)
6) Wolf et al. (1983)
7) Wiik (1956)
8) Lodders et al. (1993)
9) Müller and Zähringer (1966)
10) Djakonowa and Charitonowa (1960)
11) Binns (1969)
12) Jarosewich (1967)
13) Calculated from data of Watters and Prinz (1979) assuming 21 wt. % metal and 79 wt. % enstatite.

Table A2. Trace element abundances (ppm) of aubrites relevant for this work.

	Rb	Sr	Y	Zr	Br	Ba	La	Ce	Nd	Th	U	References
ALH 78113	0.667	2.38				1.18	0.231	0.632	0.429			1)
Aubres	0.605							0.347	0.241			2)
Bishopville	1.91							0.371	0.216			2)
Bustee	0.63											3)
Cumberland Falls				0.64								4)
Khor Temiki				4.3	0.14	5.4						5), 12)
Mayo Belwa							0.14	0.40				6)
Mt. Egerton (silicate)								0.111	0.06			2)
Norton County	0.084	1.4		2.6		3.15						2), 4), 7), 8)
Peña Blanca Spring	0.289						0.27	1.2	0.075			2), 9)
Pesyanoe (average)	1.67											3)
(dark)	2.41			0.28								10), 2)
(light)				0.26								10)
Pesyanoe enstatite	0.134											2)
Shallowater	0.86							0.051				3), 11)
Average for Fe-poor (Fe <2%) aubrites												
	0.93	1.9		3.45	0.23	3.24	0.21	0.59	0.24			
Average given by Mason (1978). Figures in parentheses are number of meteorites analyzed.												
	1.81	1.4	2.09	0.9	0.14	2	0.21	0.81	0.63	0.028	0.0045	
	(2)	(1)	(1)	(2)	(2)	(1)	(1)	(1)	(1)	(2)	(2)	

1) Shimizu and Masuda (1981)
2) Wolf et al. (1983)
3) Biswas et al. (1980)
4) Ehmann and Rebagay (1970)
5) Burger et al. (1989)
6) Graham and Henderson (1985)
7) Von Michaelis et al. (1969)
8) De Laeter and Hosie (1978)
9) Lodders et al. (1993)
10) Laul et al. (1972)
11) Keil et al. (1989)
12) Eugster (1967)

Table A3. Results of He, Ne, and Ar measurements.

	Sample weight (mg)	^{4}He	^{20}Ne	^{40}Ar	$\frac{^{4}\text{He}}{^{3}\text{He}}$	$\frac{^{20}\text{Ne}}{^{22}\text{Ne}}$	$\frac{^{22}\text{Ne}}{^{21}\text{Ne}}$	$\frac{^{36}\text{Ar}}{^{38}\text{Ar}}$	$\frac{^{40}\text{Ar}}{^{36}\text{Ar}}$
			10^{-8}cm^{3}STP/g						
ALH 84007,95	20.10	295 ± 9	13.8 ± 0.4	69.8 ± 5.0	6.11 ± 0.06	0.863 ± 0.016	1.075 ± 0.011	1.00 ± 0.10	304 ± 20
ALH 84024,11	20.72	200 ± 6	9.54 ± 0.30	92.0 ± 5.0	7.43 ± 0.08	0.950 ± 0.010	1.089 ± 0.011	2.09 ± 0.12	249 ± 20
	30.13	114 ± 3	7.22 ± 0.30	60.0 ± 3.5	7.12 ± 0.07	0.898 ± 0.010	1.084 ± 0.012	1.80 ± 0.10	229 ± 17
	20.04	162 ± 5	7.65 ± 0.25	67.5 ± 6.0	6.97 ± 0.12	0.887 ± 0.010	1.067 ± 0.011	1.82 ± 0.20	225 ± 20
	20.44	180 ± 6	8.87 ± 0.25	73.4 ± 6.0	6.85 ± 0.07	0.878 ± 0.009	1.063 ± 0.011	1.83 ± 0.17	218 ± 20
ALH 84024,15	21.41	171 ± 5	8.87 ± 0.25	53.8 ± 5.0	6.05 ± 0.07	0.837 ± 0.016	1.079 ± 0.020	1.66 ± 0.25	314 ± 40
ALH 84024	average	165 ± 20	8.43 ± 0.70	69.3 ± 10.0	6.88 ± 0.40	0.890 ± 0.30	1.079 ± 0.010	1.84 ± 0.10	247 ± 30
EET 90033,7	21.17	782 ± 24	45.6 ± 2.0	1350 ± 55	12.0 ± 0.1	1.90 ± 0.02	1.19 ± 0.01	1.86 ± 0.03	690 ± 20
	32.10	351 ± 11	27.7 ± 0.8	1206 ± 40	13.2 ± 0.1	1.58 ± 0.02	1.17 ± 0.02	1.89 ± 0.03	904 ± 20
	20.61	773 ± 23	52.40 ± 1.6	1654 ± 55	15.5 ± 0.2	2.24 ± 0.02	1.18 ± 0.02	2.08 ± 0.04	757 ± 20
	21.17	593 ± 18	43.9 ± 1.4	1521 ± 50	14.8 ± 0.2	2.10 ± 0.02	1.19 ± 0.02	2.15 ± 0.04	723 ± 20
	average	625 ± 110	42.4 ± 5.0	1433 ± 90	13.9 ± 0.2	1.96 ± 0.15	1.18 ± 0.01	2.00 ± 0.07	768 ± 45
EET 90757,9	21.51	74.4 ± 2.0	15.9 ± 0.7	263 ± 10	6.70 ± 0.08	0.855 ± 0.010	1.123 ± 0.020	1.04 ± 0.04	490 ± 25
	30.13	71.6 ± 2.0	15.9 ± 0.5	289 ± 10	6.63 ± 0.07	0.870 ± 0.015	1.098 ± 0.011	1.02 ± 0.03	580 ± 20
	average	73.0 ± 2.0	15.9 ± 0.5	276 ± 13	6.66 ± 0.07	0.862 ± 0.010	1.110 ± 0.013	1.03 ± 0.03	535 ± 45
LEW 87007,11	20.19	193'000 ± 16'000	461 ± 18	13'200 ± 1'000	1'063 ± 12	6.52 ± 0.07	2.15 ± 0.03	3.68 ± 0.05	1'060 ± 40
	31.74	114'100 ± 3'500	359 ± 11	5'710 ± 200	1'027 ± 11	6.08 ± 0.06	2.00 ± 0.02	3.42 ± 0.04	566 ± 10
	5.48	145'500 ± 6'500	399 ± 17	7'890 ± 250	969 ± 10	6.32 ± 0.06	1.97 ± 0.03	3.18 ± 0.08	675 ± 20
	4.99	148'800 ± 12'000	425 ± 13	7'410 ± 250	965 ± 10	6.22 ± 0.07	1.98 ± 0.02	3.42 ± 0.10	622 ± 15
	average	150'400 ± 16'000	411 ± 20	8'550 ± 1'700	1'006 ± 25	6.29 ± 0.08	2.02 ± 0.04	3.42 ± 0.09	731 ± 110
Pesyanoe enstatite crystal 1	15.14	1'199 ± 40	22.8 ± 0.7	111.8 ± 7.0	15.3 ± 0.2	0.951 ± 0.017	1.106 ± 0.012	1.98 ± 0.10	156 ± 12
Pesyanoe enstatite crystal 2	16.41	550 ± 17	19.9 ± 0.6	247 ± 10	7.10 ± 0.07	0.862 ± 0.010	1.116 ± 0.020	1.20 ± 0.07	492 ± 30
Pesyanoe-90.2	24.53	853'600 ± 48'400	4'290 ± 130	4'620 ± 140	2'605 ± 145	11.07 ± 0.11	8.91 ± 0.09	4.94 ± 0.05	30.9 ± 0.3
QUE 97280,7	20.75	830 ± 25	17.7 ± 0.5	2'232 ± 70	11.6 ± 1.4	0.873 ± 0.010	1.036 ± 0.011	3.36 ± 0.04	288 ± 6
QUE 97348,6	20.59	190 ± 6	14.8 ± 0.5	2'246 ± 70	7.38 ± 0.08	0.970 ± 0.009	1.029 ± 0.011	3.02 ± 0.06	345 ± 8
Y 793592,86	20.88	9'040 ± 350	172 ± 5	5'241 ± 160	94.8 ± 0.9	3.49 ± 0.04	1.38 ± 0.02	2.64 ± 0.04	1123 ± 20
	20.20	8'072 ± 300	160 ± 5	5'322 ± 160	101.1 ± 1.0	3.49 ± 0.04	1.38 ± 0.01	2.61 ± 0.04	1134 ± 20
	average	8'556 ± 400	166 ± 5	5'282 ± 160	98.0 ± 1.0	3.49 ± 0.04	1.38 ± 0.02	2.62 ± 0.04	1128 ± 20

Table A4. Aubrite analyses of other workers from the compilation of Schultz and Franke (2000).

	Reference	^{4}He	^{20}Ne	^{40}Ar	^{4}He	^{20}Ne	^{22}Ne	^{36}Ar	^{40}Ar
		10^{-8}cm^{3}STP/g			^{3}He	^{22}Ne	^{21}Ne	^{38}Ar	^{36}Ar
ALH 78113	1)	427	10.6	1'220	12.00	0.845	1.090	1.45	1'584
ALH 84007	2)	338	12.67	330	8.00	0.850	1.090	2.33	524
ALH 84008	2)	313	8.06	620	12.08	0.851	1.100	2.36	939
ALH 84011	2)	295	11.23	400	8.17	0.844	1.090	2.79	597
Aubres	3)	208	5.50	454	15.07	0.833	1.119	2.11	1'195
Bishopville	4), 5)	638	21.3	5'370	6.95	0.854	1.112	1.58	9'944
Bustee	3), 6)	7'800	143	1'860	86.2	3.73	1.468	2.08	516
Cumberland Falls Fe-poor	3), 5), 7)	309	27.0	573	10.6	0.853	1.091	1.52	474
Cumberland Falls Fe-rich	5)	430	24.5	1'425	17.6	0.914	1.094	2.00	509
Khor Temiki enstatite	8)	500	21.4	220	5.41	0.786	1.122	1.31	863
Mayo Belwa	9)	1'825	47.2	8'250	10.25	0.807	1.129	1.07	3'784
Norton County	4), 5), 10)	1'544	52.0	470	7.52	0.869	1.099	0.794	272
Pena Blanca Spring	5)	1'090	24.7	650	9.16	0.837	1.185	1.25	650
Pesyanoe light	11)	2'680	24.5	173	30.5	1.109	1.122	1.71	171
Pesyanoe dark	11)	1'068'000	3'610	4'620	2'507	11.5	14.8	5.33	17.0
Shallowater	3)	277	7.90	2'010	6.30	0.868	1.197	5.34	99

For data selection criteria see text. For each meteorite average values were calculated. References: 1) Vogt et al. (1986); 2) Herpers et al. (1995); 3) Eberhardt et al. (1965a); 4) Levsky (1972); 5) Müller and Zähringer (1969); 6) Poupeau et al. (1974); 7) Zähringer (1968); 8) Eberhardt et al. (1965c); 9) Heusser et al. (1978); 10) Herzog et al. (1977); 11) Müller and Zähringer (1966).

Table A5. Results of Kr measurements.

	^{86}Kr	^{78}Kr	^{80}Kr	^{82}Kr	^{83}Kr	^{84}Kr	^{83}Kr$_c$	^{80}Kr$_n$		^{83}Kr$_c$age
	10^{-12}cm^{3}STP/g		^{86}Kr = 100			10^{-12}cm^{3}STP/g		10^{-12} cm^{3}STP/g	$(^{80}$Kr/^{82}Kr)$_n$	Ma
Norton County	19 ± 3	4.57 ± 0.18	25.4 ± 0.7	8 ± 3	86 ± 3	343 ± 15	3 ± 0.6			106
Cumberland Falls	20 ± 3	3.62 ± 0.13	94 ± 1.2	100.3 ± 2.6	74.8 ± 2.7	324 ± 13	1.94 ± 0.29	15.3 ± 2.3	2.7 ± 0.4	53 ± 12
Mount Egerton	26 ± 4	2.1 ± 0.06	13.6 ± 0.4	65.7 ± 1.7	65.1 ± 1.9	323 ± 9				
Mayo Belwa	26 ± 4	3.86 ± 0.09	26.8 ± 0.5	79.1 ± 1.5	80.1 ± 1.5	340 ± 7	3.8 ± 0.6	1.5 ± 0.2		105 ± 23
Shallowater	308 ± 46	2.04 ± 0.02	16.62 ± 0.19	67.7 ± 0.6	65.9 ± 0.6	325 ± 3	2.2 ± 0.3	10.8 ± 1.6	1.7 ± 0.8	59 ± 13